BENDING-TWIST COUPLING MECHANISM BY ELASTIC INSTABILITY: AEROELASTIC STUDY

F. Runkel[1], U. Fasel[1], G. Molinari[1], A. F. Arrieta[2], P. Ermanni[1]

[1]Laboratory of Composite Materials and Adaptive Structures, ETH Zurich, Leonhardstrasse 21, 8092 Zurich, Switzerland
Email: runkelf@ethz.ch
[2]School of Mechanical Engineering, Purdue University, 585 Purdue Mall, West Lafayette, IN, USA
Email: aarrieta@purdue.edu

Keywords: Shape Adaptation, Buckling, Bending–Twisting-Coupling, Aeroelastic Coupling

Abstract

This paper presents a purely passive morphing mechanism for wings which exploits local elastic instabilities to achieve spanwise continuous twist variations. The considered structures comprise a wingbox with two spars, one of which is designed to undergo controlled instability. The onset of buckling and the postbuckling behaviour of the wing structure are tailored by exploiting the material anisotropy of fibre–reinforced composites. When the critical buckling load is exceeded, the spar undergoes diagonal tension, in turn leading to a reduction of its effective shear stiffness. This affects the torsional compliance of the wing and changes the shear centre location, resulting in a different torsional response. Parametric studies, performed using 3–D aeroelastic analysis techniques, permit to assess the influence of various design parameters on the resulting buckling-induced change in twist. A noteworthy application for this morphing technique is represented by passive load alleviation, exploiting the aerodynamic forces to achieve the desired twist variation and consequently reducing the overall lift.

1. Introduction

Conformal shape adaptation has the potential of increasing the structural efficiency of aerospace systems by achieving optimal performance across a wide range of operational conditions [1–3]. In particular, the bending–twisting coupling of wings is one of the most decisive factors influencing the aeroelastic behaviour of such systems [4, 5]. Previous projects aimed to achieve variations in the wing twist, using both conventional internal mechanisms, such as moveable wing spars, as well as smart materials with variable stiffness have been investigated [6, 7].

Following a passive approach, we investigate the possibility to achieve a twisting shape adaptation for wing structures, accomplished by exclusively relying on the external aerodynamical loads. The underlying concept presented by the authors in [8] is based on deliberately triggering elastic instabilities in thin–walled composite beam structures. The effects resulting from buckling, namely the change in effective stiffness, are utilised to achieve a desired twisting shape adaptation mechanism. This paper extends the aforementioned conceptual investigation from simple beam structures to realistic wings under aerodynamical loads by utilising a composite beam as the load–carrying wingbox. Parametric studies, performed by means of 3–D aeroelastic analyses, enable to explore the wide space of design parameters influencing this shape adaptation mechanism, such as the fibre orientation and thickness of the buckling component, structural stiffness of the ribs, and the wingspan. The occurrence of instability enables desired airfoil nose–down effects, modifying the aerodynamic characteristics of the wing structure. The

Excerpt from ISBN 978-3-00-053387-7

achievable change in angle of attack leads to a sectional variation in the lift coefficient. This purely passive morphing mechanism can therefore be used for load alleviation, such as decreasing the root bending moment by redistributing the aerodynamic loads, thus increasing the structural efficiency of lift generating lightweight systems.

2. Morphing Concept

The structural concept on which the proposed morphing wing is based has been introduced, for the simplified case of a rectangular thin–walled composite beam, by the authors in [8]. Figure 1a shows the operation of the concept, achieving twisting of beam–like structures by purely passively inducing local elastic instabilities [8]. The presented methodology is based on designing one shear web of the beam such that it deliberately undergoes instability at a prescribed level of external loading, developing a diagonal tension field in the postbuckling regime. The onset of buckling defines the transition between two distinctive structural responses: the linear prebuckling and the nonlinear postbuckling regime. The postbuckling response, namely the reduction in effective shear stiffness of the web undergoing buckling, results in a displacement Δ of the shear centre of the section, creating a buckling–induced torsional moment acting on the structure (Figure 1a). Additionally, the torsional stiffness of the structure is decreased, augmenting the twisting deformation mechanism.

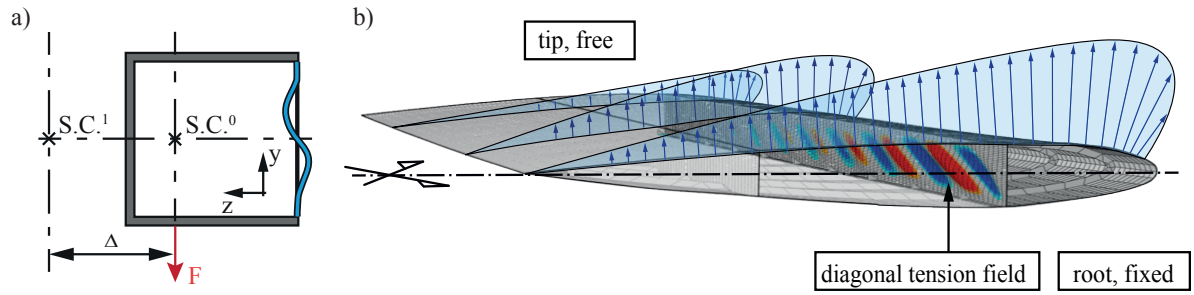

Figure 1. a) Thin-walled structure with one shear web undergoing instability. Buckling-induced shear centre relocation Δ b) Wing structure with qualitative drawing of the three-dimensional aerodynamic loads

This study extends the previous investigation to realistic wing structures, subjected to aerodynamic loads. For this purpose, a wingbox comprised by two spars and two flanges is utilised as the load–carrying component of the wing, the other components of which are a front section and rear section (see Figure 2). To achieve significant variations in twist of the entire wing, the structural response must be dominated by the stiffness of the morphing wingbox. Consequently, the torsional stiffness of the leading and trailing edge sections is reduced by means of a slot in spanwise direction.
Figure 2a shows the wing section and its components. The dimensions of the presented structure are given in Table 1. To prevent large local shape deformations of the front and rear sections, a number of ribs are distributed with uniform spacing in spanwise direction. As the ribs contribute significantly to the bending stiffness of the wing structure about the x–axis, they affect the development of the buckling in the spar. For this reason, the rib properties need to be considered in the design of the postbuckling response of the structure [8]. The wing is assumed to be manufactured out of fibre–reinforced materials, using the lay–ups and materials listed in Tables 2 and 3.

Excerpt from ISBN 978-3-00-053387-7

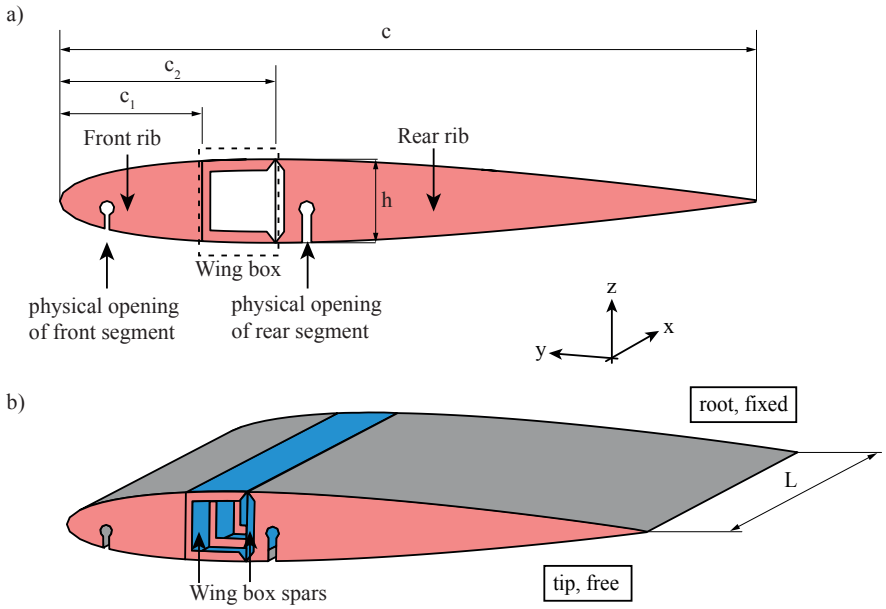

Figure 2. Structural model. Wing box coloured in blue, front and rear skin coloured in grey. Ribs coloured in red.

Table 1. Wing geometry (geometrical properties as defined in Figure 2)

Property	Symbol	Unit	Value
Airfoil chord	c	m	0.5
Airfoil length	L	m	2.5
Front spar position	c_1	m	
Rear spar position	c_2	m	
Wing box height	h	m	≈ 0.06
Wing box width	$w = c_2 - c_1$	m	0.05
Rib thickness	t_R	m	0.001
Number of ribs			6

Table 2. Material properties[a]

Property	Unit	CFRP	GFRP
E_1	GPa	135	25
E_2	GPa	10	25
G_{12}	GPa	5	4
ν_{12}		0.3	0.2

[a]Lamina of CM-Preg T-C- 120/625 CP002 35 prepreg (CFRP) [9] and glass weave VE 106 (GFRP) [10] [11].

Table 3. Lay–Ups of structural model[a]

Component	thickness	Lay–Up
Wingbox	$t_C = 1.5$ mm	$[0^\circ_C; 90^\circ_C]_{sym}$
Front and rear skin	$t_S = 1.5$ mm	$[0^\circ_C; 90^\circ_C]_{sym}$
Buckling web	t_W	$[\beta_C]$
Ribs	$t_R = 1$ mm	

[a]For component definition, see Figure 2, subscript C stands for material CFRP

Excerpt from ISBN 978-3-00-053387-7

3. Aeroelastic Analysis Technique

The structural response resulting from the application of the aerodynamic loads leads to a change in twist along the span. In turn, this causes a significant variation of the aerodynamic forces. To properly simulate for this bi–directional interaction, a weakly–coupled fluid–structure analysis technique is utilised. Figure 3 describes this methodology with a flow chart.

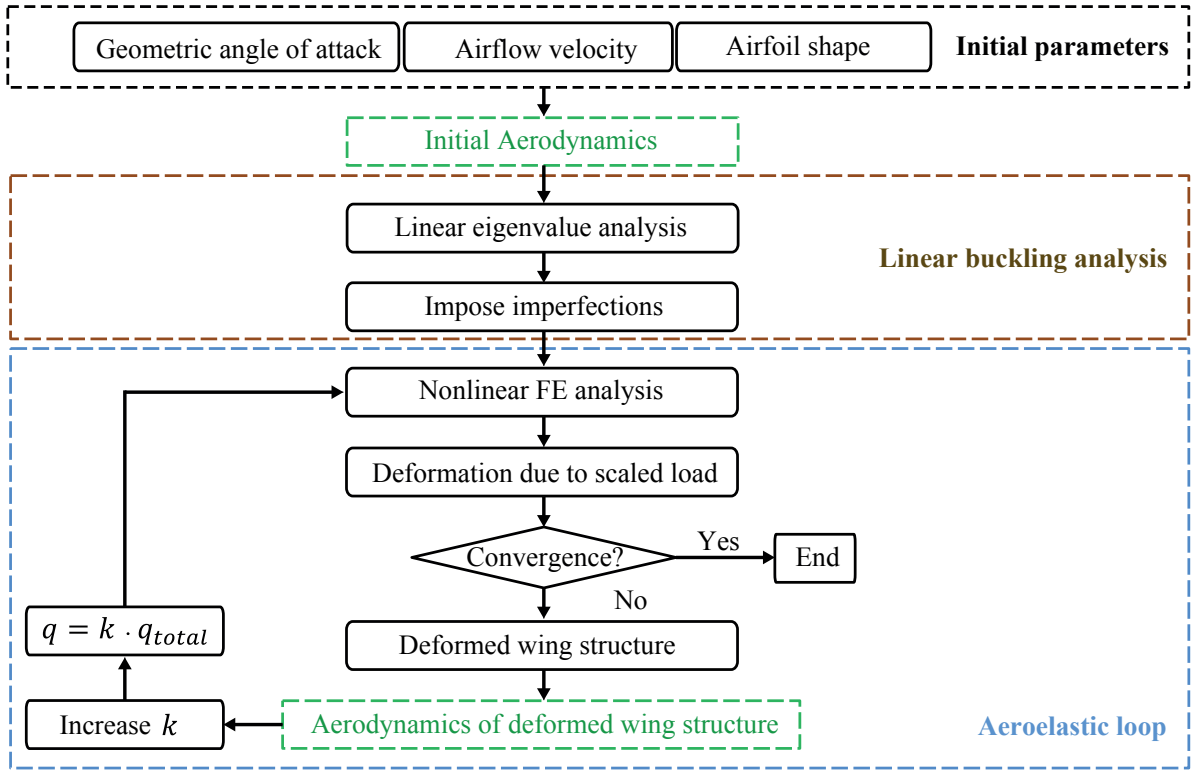

Figure 3. Aeroelastic analysis consisting of initial aerodynamics, linear buckling analysis and an the aeroelastic loop representing the buckling–induced shape adaptation under aerodymic loads

In each iteration loop, the three–dimensional aerodynamics are computed utilising Weissinger's nonlinear lifting–line method [12]. For this purpose, the wing is subdivided in a number of spanwise sections, at which the airfoil shape is extracted. For each of these profiles, the lift is calculated – as a function of the angle of attack – by means of XFOIL [13], considering viscous phenomena. This information is used in Weissinger's nonlinear lifting line method, resulting in the determination of the effective angle of attack for each section. Utilising XFOIL, the chordwise pressure distribution is computed for each spanwise section at the effective angle of attack, and interpolated on the entire wing surface. A finite element analysis is performed to assess the linear buckling response of the wing structure when subjected to the intial pressure field. Furthermore, this analysis provides the critical buckling load, leading to the onset of instability[1]. In addition, the structural stability of the rest of the structure for the given loads is verified. Geometric imperfections are then imposed onto the structural model by superposing the shape functions obtained from the eigenvalue analysis.
The structural model with the imposed imperfections is analysed through a geometrically nonlinear static finite element analysis. The applied load is the aerodynamic pressure scaled with a factor $0 < k < 1$. The deformation of the wing caused by the scaled load is assessed, and the new total pressure load on the wing is calculated with Weissinger's nonlinear lifting line method. The scaling factor k is increased,

[1] Assuming constant aerodynamic loads

Excerpt from ISBN 978-3-00-053387-7

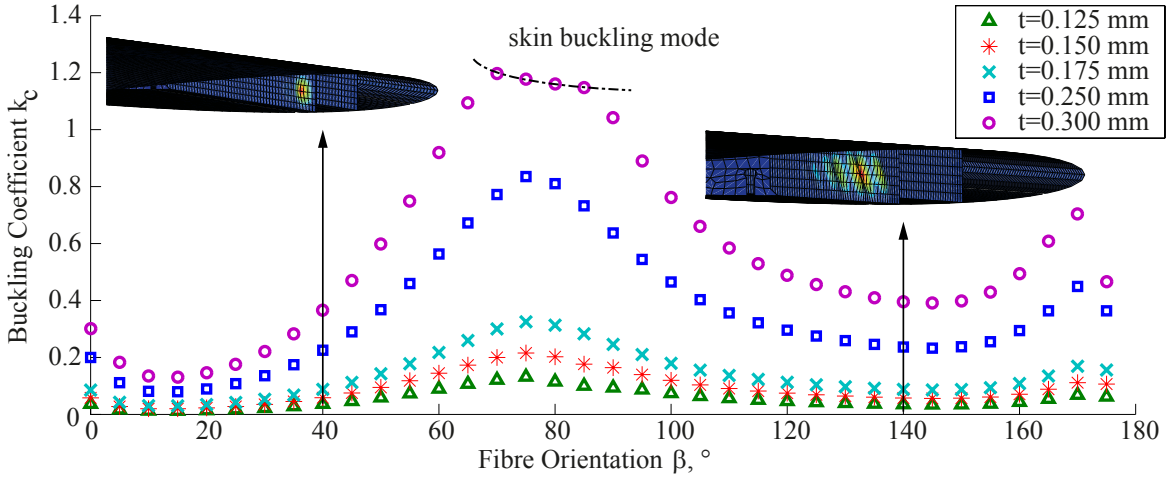

Figure 4. Buckling Coefficients as a function of the fibre angle. For fibre angles $\beta = 40\,°$ and $\beta = 140\,°$ the obtained buckling modes are shown.

and the loop is repeated until the scaling factor reaches $k = 1$ and further convergence criteria, such as a maximum trailing edge displacement per iteration, are fulfilled. This incremental increase in load enables to update the aerodynamic pressure field corresponding to the current deformation, considering buckling–induced effects. For all conducted studies in this paper, the initial control variable for the aeroelastic coupling is $k_{\text{init}} = 0.2$ and it is increased in each iteration step by $\Delta k = 0.2$. The linear buckling and nonlinear postbuckling analyses are conducted utilising the commercial finite element code ABAQUS Standard/FEA. For all simulations, shell elements with reduced integration S4R have been utilised. The postbuckling analyses are conducted with a nonlinear static solution procedure utilising automatic stabilization.

4. Results of Parametric Studies

4.1. Onset of Buckling

For the structural model, presented in Section 2, Figure 4 shows the result of a linear buckling eigenvalue calculation for varying fibre angles β and buckling shear web thicknesses t. It can be observed that, beside the spar thickness, also the fibre angle significantly influences the buckling load, and leads to two distinguishable buckling modes. For two particular spar designs (fibre angles $\beta = 40\,°$ and $\beta = 140\,°$), the obtained buckling shape is illustrated in Figure 4. For spars with a thickness $t = 0.3\,\text{mm}$ and fibre angles of $\beta \approx 90\,°$, buckling occurs in the wing skin instead of in the spar. The strong dependence of the critical buckling load on the fibre direction is of particular importance, as it defines the onset of the shape adaptation. Furthermore, it influences the postbuckling response, as the resulting twist angle not only depends on the change in torsional stiffness and shear centre location, but also on the external load [8].

4.2. Attainable Twist–Morphing Performance

The effects of the wing design parameters, such as buckling spar lay–up, spar thickness and thickness of the ribs, on the achievable buckling–induced twisting are assessed by means of parametric studies. For the structural model, presented in Section 2, the aeroelastic deformation is calculated according to the scheme given in Figure 3. The initial angle of attack is $\alpha = 7\,°$ and the airflow velocity is

Excerpt from ISBN 978-3-00-053387-7

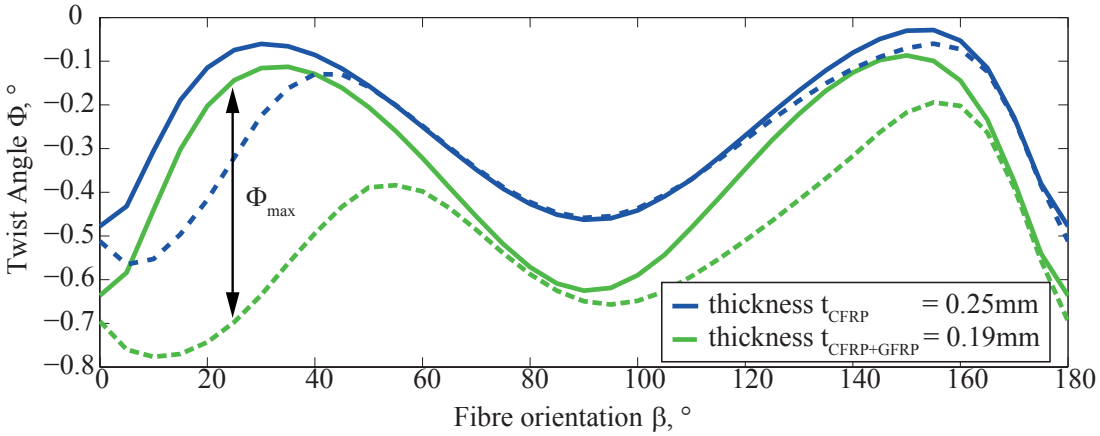

Figure 5. Twist angles at the wing tip as a function of the fibre orientation. Solid lines show results of geometrically linear calculations, dashed lines show results of geometrically nonlinear calculations.

$V_\infty = 42\,\mathrm{m/s}$. Figure 5 shows the resulting twist angles at the wing tip for a buckling web with thickness $t_W = 0.25\,\mathrm{mm}$ and varying fibre orientations β, in both the case of a linear (solid line) and a geometrically nonlinear (dashed line) calculation. The linear calculation cannot capture the occurrence of buckling and the buckling–induced change in twist angle $\Delta\Phi = \Phi_{\mathrm{Linear}} - \Phi_{\mathrm{Nonlinear}}$ can be obtained by comparing the results with the geometrically nonlinear study. At specific ranges of fibre angles ($\beta \approx 0\,° - 50\,°$ and $\beta \approx 120\,° - 160\,°$), the influence of buckling on the wing twist is pronounced while it disappears for other fibre angles. For the presented model, the maximum change in twist angle ($\Phi_{\mathrm{max}} \approx 0.3°$) is achieved for fibre orientation $\beta = 15°$.

The same analysis is conducted with a different lay–up of the buckling spar. The study is conducted for a buckling spar with thickness $t_W = 0.19\,\mathrm{mm}$. The spar consists of one layer of unidirectional CFRP embedded within two layers of GFRP weave[2] with ply thickness $t_{\mathrm{Ply,Glass}} = 0.02\,\mathrm{mm}$ (Table 2). The results for the obtained twist angle for the linear (solid line) and nonlinear (dashed line) calculations are shown in Figure 5. In comparison, the regions of high buckling–induced torsion are more pronounced, leading to a maximum change in twist of $\Phi_{\mathrm{max}} \approx 0.55°$ for the fibre orientation $\beta = 25°$. The increased influence of the local instability on the overall twisting of the wing structure is caused by the lower buckling coefficient of the wing design with the thinner buckling spar. For a similar aerodynamic pressure load, the diagonal tension field is more pronounced, leading to a larger reduction in effective shear stiffness and hence shear centre relocation and torsional stiffness. The influence of the rib thickness on the obtained twist angle is shown in Figure 6. It can be observed that the buckling–induced twist increases with decreasing rib thickness. This results from the bending stiffness of the ribs influencing the development of the diagonal tension field. For small thicknesses, the compliance of the ribs allows for larger displacements of the wingbox flanges leading to a pronounced buckling field and therefore reduction in effective shear stiffness [8].

With an airflow velocity of $V_\infty = 84\,\mathrm{m/s}$ and a wing length of $L = 1.25\,\mathrm{m}$, the change in lift coefficient with the passively achieved mechanism is shown for particular fibre orientations in Figure 6. Due to the increased aerodynamic pressure load, the resulting torsional moment on the wing is significantly larger compared to the previously studies. For this reason, the shear centre relocation and torsional compliance lead to a larger global buckling–induced change in twist. Due to the triggered nose–down mechanism, the angle of attack is reduced, resulting in a lift reduction of approximately 13%, or $\Delta c_L = 0.082$, for fibre orientations $\beta \approx 25°$. This parametric study therefore shows the possibility of utilising the proposed passive morphing mechanism for load alleviation purposes.

[2]One main axis of the weave is oriented along the fibre direction of the unidirectional carbon fibre composite midlayer.

Excerpt from ISBN 978-3-00-053387-7

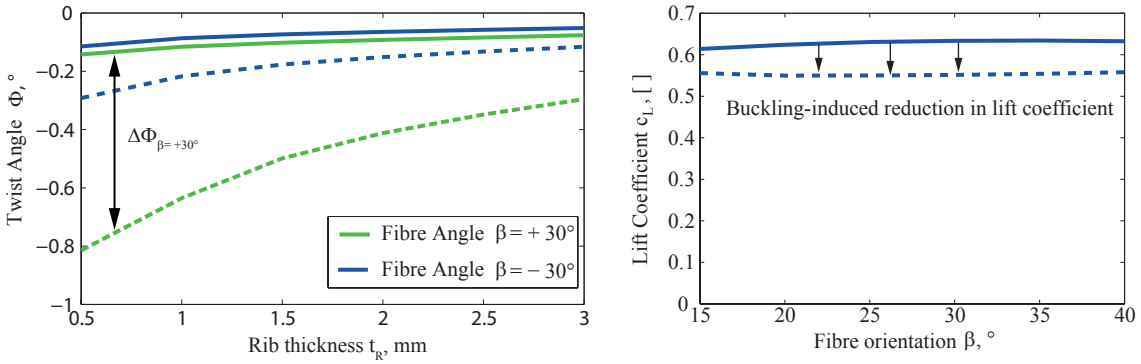

(a) Twist angle as a function of rib thickness

(b) Lift coefficient reduction as a function of the spar fibre orientation β

Figure 6. Results of parametric studies. Solid lines show results of geometrically linear calculations, dashed lines show results of geometrically nonlinear calculations.

5. Conclusion

This paper investigates a purely passive twisting morphing mechanism for wing structures. The design exploits the material anisotropy provided by composite materials, such that local elastic instability occurs in one wingbox spar at a desired level of external loading. Postbuckling of the spar changes its effective shear stiffness, resulting in a shear centre relocation and variation of torsional compliance of the wing structure. These structural changes lead to a twisting response of the wing, achieved purely passively by the utilisation of the external aerodynamic forces.
Aeroelastic analyses are conducted for different wing designs to obtain the achievable buckling–induced change in twist for wing structures under realistic aerodynamic loading. The lever arm between the centre of pressure of the airfoil and the shear centre determines the resulting torsional moment triggering the shape adaptation. Therefore, the initial shear centre location of the wing structure also has a great influence on this morphing mechanism as it determines whether the lever arm of the torsional moment is increased or reduced in the postbuckling regime. For all studies presented in this paper, the initial shear centre is located ahead of the centre of pressure such that the external loads lead to a nose–down twisting of the wing in the prebuckling regime. Buckling of the rear spar, located behind the initial shear centre, leads to a relocation of the shear centre closer to the wing nose. For this reason, buckling of the rear spar attenuates the nose–down twisting response, leading to a reduction in the angle of attack of the wing. Parameters, such as fibre orientation and thickness of the spar undergoing instability, stiffness of the ribs, and airflow velocity, are investigated to tailor the wing structure for a desired postbuckling response. The study shows the large influence of particular design parameters on the proposed morphing technique, while a failure analysis, particularly interesting in the spar for loads exceeding significantly the buckling load, and a study of the fatigue behaviour go beyond the scope of this work. Reducing the angle of attack by achieving a nose–down twisting of wing structures shows potential to reduce the lifting force acting on wing structures and consequently the resulting root bending moment. For one particular wing design, the lift of the wing could be reduced by approximately 13 %, or $\Delta c_L = 0.082$. Therefore, the proposed concept is especially beneficial for load alleviation purposes, offering potential to augment the structural efficiency of lightweight systems by achieving desired shape changes, only triggered by external aerodynamic loads.

Excerpt from ISBN 978-3-00-053387-7

Acknowledgments

We gratefully acknowledge the support of the European Office of Aerospace Research & Development (EOARD) Grant Number FA8655-13-1-3057 "Variable Stiffness Wing Structures with Compliance for Aeroelastic Morphing".

References

[1] D. J. Wagg, I. P. Bond, P. M. Weaver, and M. I. Friswell, editors. *Adaptive Structures: Engineering Applications*. John Wiley & Sons, Ltd, 2007.

[2] Terrence A. Weisshaar. Morphing Aircraft Systems: Historical Perspectives and Future Challenges. *Journal of Aircraft*, 50(2):337–353, 2013.

[3] Giulio Molinari, Andres F. Arrieta, and Paolo Ermanni. Aero-Structural Optimization of Three-Dimensional Adaptive Wings with Embedded Smart Actuators. *AIAA Journal*, 52(9):1940–1951, September 2014.

[4] W. Raither, A. Bergamini, and P. Ermanni. Profile beams with adaptive bending-twist coupling by adjustable shear centre location. *Journal of Intelligent Material Systems and Structures*, 24(3):334–346, August 2012.

[5] T. A. Shirk, M. H., Hertz, T. J., Weisshaar. Aeroelastic tailoring - Theory, practice, and promise. *Journal of Aircraft*, 23(1):6–18, 1986.

[6] R M Ajaj, M I Friswell, D D Smith, G Allegri, a T Isikveren, Aircraft Concepts, Deputy Chief, and Technical Officer. Roll Control of a UAV Using an Adaptive Torsion Structure. *Aerospace Engineering*, (April):1–15, 2011.

[7] Wolfram Raither, Matthias Heymanns, Andrea Bergamini, and Paolo Ermanni. Morphing wing structure with controllable twist based on adaptive bending twist coupling. *Smart Materials and Structures*, 22(6):065017, June 2013.

[8] F. Runkel, A. Reber, G. Molinari, A.F. Arrieta, and P. Ermanni. Passive twisting of composite beam structures by elastic instabilities. *Composite Structures*, 147:274 – 285, 2016.

[9] CM-Preg T-C- 120/625 CP002 35 Property Data Sheet.

[10] Suter Kunststoffe AG. Data sheet and product information: Glas-Fabrics. Technical report, Suter Kunststoffe AG, Fraubrunnen, Switzerland, 2015.

[11] Amanda Caulder. Mechanical Properties of Carbon Fiber Composite Materials, Fiber / Epoxy resin (120C Cure). Technical report, ACP Composites, Inc., Livermore, CA, 2014.

[12] DB Owens. Weissinger's model of the nonlinear lifting-line method for aircraft design. In *36th Aerospace Sciences Meeting and Exhibit*, Reno, NV, jan 1998. AIAA.

[13] M. Drela. *XFOIL 6.9 User Primer*. 2001.

Excerpt from ISBN 978-3-00-053387-7